AIChE

A New Framework and a Simpler Method for the Development of Batch Crystallization Recipes

Jeffrey D. Ward and Cheng-Ching Yu
Dept. of Chemical Engineering, National Taiwan University, Taipei 106-07, Taiwan

Michael F. Doherty
Dept. of Chemical Engineering, University of California, Santa Barbara, CA 93106

DOI 10.1002/aic.12284
Published online September 7, 2010 in Wiley Online Library (wileyonlinelibrary.com).

We use a new generalized dimensionless model of a seeded batch crystallization process to compare results from four crystal growth rate/concentration trajectories: a numerically-computed optimal trajectory, a constant growth rate trajectory, a trajectory proposed by Mullin and Nyvlt that can be calculated without a kinetic model, and a linear concentration-time trajectory. Because the model is generalized and dimensionless it is not specific to any particular solute–solvent system. We show that if seed properties are good, all trajectories achieve a good result, whereas if seed properties are poor all trajectories achieve a poor result. If seed properties are intermediate, the linear concentration trajectory performs much worse than the other trajectories. On the basis of this, we conclude: (1) Linear trajectories and natural cooling trajectories are poor and should be avoided. When evaluating the benefit derived from an optimization of a temperature/saturation concentration trajectory, the appropriate benchmark should be the Mullin-Nyvlt trajectory, which typically performs much better than the linear trajectory and can be calculated knowing only the mass of seeds at the beginning of the batch. (2) Changing seed properties is more likely to improve batch crystallizer performance than optimizing the growth/saturation concentration trajectory. (3) For rapid process development, the most reasonable approach is to use the Mullin-Nyvlt trajectory and seek to improve process performance by adjusting seed properties. *AIChE J,* 57: 606–617, 2011
Keywords: crystallization, optimization, particle technology, process control, solids processing

Introduction

Crystallization is a vital unit operation in the chemical and related industries. Although some large-scale processes operate with continuous crystallizers, the vast majority of crystallization processes in industry are operated batch-wise. The vast majority of batch crystallization processes are charged with seeds at the beginning of the batch to improve performance. Such a process is termed a seeded batch crystallization process.

The driving force for crystallization is the supersaturation of the solution. Batch crystallization processes have an external mechanism that induces a certain supersaturation

Additional Supporting Information may be found in the online version of this article.

Correspondence concerning this article should be addressed to J. D. Ward at jeffward@ntu.edu.tw.

in the solution; this supersaturation drives the growth of crystals in the suspension and generally also causes the formation of new small particles by nucleation. Supersaturation can be induced by a variety of methods, including cooling, solvent evaporation, introduction of antisolvent, etc.

Because the process is operated batch-wise, the question naturally arises, how should the supersaturation vary as a function of time? This question is equivalent to asking, how should the crystallizer temperature (or solvent evaporation rate, etc.) change with time? A number of researchers have attempted to answer this question by formulating a continuous optimization problem, beginning with Jones[1] in 1974. (The number of such publications is too great to permit a comprehensive review here. See Rawlings et al.[2] and Ward et al.[3] and references therein.) Experimental data are used to develop a mathematical model of the kinetics of nucleation and growth for a particular solute–solvent system of interest. Then an objective function is developed, usually on the basis of desired overall crystal size distribution at the end of the batch. Finally, a continuous optimization algorithm is developed to compute the optimal trajectory. Alternatively, Vollmer and Raisch[4,5] showed that the conventional model for a batch crystallization has the property of orbital flatness, which means that it is possible to determine whether a given desired final product CSD is feasible, and if so what input trajectory will lead to the desired result. Whereas these methods in principle can give the optimal result, they have two drawbacks. One is that it may be very time-consuming to develop a kinetic model, and the kinetic model may not be robust to changes in vessel geometry as during scale-up, etc. The other drawback is that the result is only valid for the particular crystal–solvent system that was investigated and sheds little light on the general problem or the nature of its solution.

An alternative method is to assume that it is optimal (or nearly optimal) to operate with constant supersaturation over the course of the batch. Several arguments can be made to support this assumption, although none is mathematically rigorous: (1) As both nucleation and crystal growth increase with increasing supersaturation, operating with constant supersaturation seems like a "fair" or "reasonable" tradeoff between the two effects. (2) Regardless of the exact shape of the supersaturation trajectory, it is definitely desirable that the metastable zone width not be exceeded at any point in the trajectory; the metastable zone width is least likely to be exceeded if the process is operated with constant supersaturation as at any point where the supersaturation exceeds the time-average supersaturation it is closer to the metastable zone boundary than necessary. Operation with constant supersaturation can be achieved either by developing a process model and solving for the trajectory that is expected to give a constant supersaturation, or by measuring or estimating the supersaturation online and adjusting the temperature via feedback control.

It turns out that under a restricted set of conditions, it is possible to solve analytically for the concentration trajectory that will achieve constant supersaturation. This was first done by Mullin and Nyvlt,[6] who published analytical expressions for the solution concentration for the case of unseeded batch crystallization with nucleation at a constant rate and for the case of seeded batch crystallization where nucleation is negligible. As almost all crystallization processes employ seeds, the latter case is more useful and typically offers a significant improvement over linear or natural cooling trajectories. The Mullin-Nyvlt trajectories have the great advantage that they can be calculated without a model for the kinetics of nucleation and growth, which is almost never available in industrial practice. In spite of this, most researchers who determine optimal trajectories compare the results of the optimization with the inferior linear or natural cooling trajectories.

A further consideration in the operation and optimization of seeded batch crystallization is the effect of seed properties on the outcome, and the effect that seed properties may have on the shape of the optimal supersaturation trajectory. Several authors have published reports that optimizing seed properties can improve the outcome dramatically and may be more important than optimizing the supersaturation trajectory.[7–9] However, these results are reported for specific case study systems and it is not clear to what extent they are valid in the general case.

In this contribution, we report optimized supersaturation and concentration trajectories for a generic nondimensionalized seeded batch crystallization process. We also compare the results with the result obtained using a constant growth rate trajectory, the Mullin-Nyvlt trajectory, and a linear concentration trajectory. Because the process model is generic and nondimensional, we can explore a wide range of parameter space and seed properties and draw general conclusions that are not limited to any particular solute–solvent system or crystallizer geometry. Furthermore, because we consider the Mullin-Nyvlt trajectory as well as the linear concentration trajectory, we can provide a more fair and accurate estimate of the marginal improvement in process performance that can be achieved if the engineer undertakes the difficult and time-consuming task of developing a kinetic model. If the Mullin-Nyvlt trajectory performs nearly as well as the optimal trajectory or constant growth rate trajectory, it would probably be preferred because it can be implemented without a kinetic model for nucleation and growth or online supersaturation measurement.

Model Development

This section presents a summary of the development of the dimensionless model for the operation of a seeded batch crystallizer that is used in this work. A complete derivation of the model is provided in the web-published supplement to this article. The method of moments is originally due to Hulbert and Katz.[10] Additional background information is available in reference texts.[11–15]

In the absence of agglomeration and breakage, a general statement of the population balance for a well-mixed batch crystallization system is:

$$\frac{\partial f(L,t)}{\partial t} + \frac{\partial (G(L,t) f(L,t))}{\partial L} = 0 \tag{1}$$

where $f(L, t)$ is the crystal size distribution (CSD) function, B is the nucleation rate (#/m^{3}s) and G is the crystal growth rate

(m/s). Equation 1 is subject to an initial condition based on the properties of the seeds at the beginning of the batch, and to a left boundary condition:

$$f(0,t) = \frac{B(f(L,t),t)}{G(0,t)} \tag{2}$$

The driving force for both nucleation and growth is the supersaturation:

$$S = C - C_{\text{sat}} \tag{3}$$

Common forms for the expressions for crystal growth rate and secondary nucleation are:

$$G = k_g S^g \tag{4}$$

$$B = k_b G^\gamma \mu_3 \tag{5}$$

where k_g, g, k_b and γ are empirically determined kinetic parameters and μ_3 is the third moment of the CSD. The moments of the CSD are determined according to:

$$\mu_i = \int_0^\infty L^i f(L) dL \quad i = 0, 1, 2, \ldots \tag{6}$$

And it can be shown (if the crystal growth rate is independent of size) that:

$$\frac{d\mu_0}{dt} = B \tag{7}$$

$$\frac{d\mu_i}{dt} = iG\mu_{i-1} \quad i = 1, 2, \ldots \tag{8}$$

A mass balance on the solute shows that the time rate of change of the solution concentration, C, is given by:

$$\frac{dC}{dt} = -3G\rho_c k_v \mu_2 \tag{9}$$

where ρ_c and k_v are the crystal density and crystal volumetric shape factor, respectively. The initial values of the moments are given by the seed properties and the initial concentration is the initial solution concentration.

Generally, it is desired to reduce the solution concentration from some initial value C_0 to some final value C_f in some fixed batch time t_f. This is accomplished by reducing the saturation concentration C_{sat} in some predetermined manner as a function of time.

It is desirable to keep track of the nucleated crystals (subscript n) separately from the seed-grown crystals (subscript s). In this case, for the seed-grown crystals, we can say:

$$\frac{d\mu_{s,0}}{dt} = 0 \tag{10}$$

$$\frac{d\mu_{s,i}}{dt} = iG\mu_{s,i-1} \quad i = 1, 2, \ldots \tag{11}$$

And for the nucleus-grown crystals, we can write:

$$\frac{d\mu_{n,0}}{dt} = B \tag{12}$$

$$\frac{d\mu_{n,i}}{dt} = iG\mu_{n,i-1} \quad i = 1, 2, \ldots \tag{13}$$

Note that:

$$\mu_i = \mu_{s,i} + \mu_{n,i} \tag{14}$$

Equations 9–13 form a set of coupled ordinary differential equations. The initial values of the moments of the nucleus-grown crystals are zero, and the initial values of the moments of the seed-grown crystals are given by the initial properties of the seeds. If the initial seed properties are specified and the saturation concentration is specified as a function of time, then Eqs. 9–13 can be solved simultaneously together with the kinetic expressions for crystal nucleation and growth rates to determine the moments of the seed-grown and nucleus-grown crystals at the end of the batch.

Typically, an objective function is formulated based on the moments of the seed-grown and nucleus-grown crystals at the end of the batch, and a continuous optimization method is employed to solve for the saturation concentration (or temperature) trajectory that minimizes (or maximizes) the objective. Ward et al.[3] discussed the influence of the objective function on the qualitative shape of the optimal trajectory. For this study, we consider only a single objective, which is to minimize the mass of the nucleus-grown crystals at the end of the batch. As the initial and final solute concentrations are fixed (which means that all trajectories have the same total solids production rate), this objective is equivalent to maximize the mass or the average size of the seed-grown crystals.

With a suitable choice of dimensionless variables (see the web-published supplement), the model can be expressed as:

$$\frac{d\mu_0'}{dt'} = B' = (G')^\gamma \mu_3' \tag{15}$$

$$\frac{d\mu_i'}{dt'} = iG'\mu_{i-1}' \quad i = 1, 2, 3 \tag{16}$$

The same treatment can also be applied to $\mu_{s,i}$ and $\mu_{n,i}$ separately.

For the case where the crystallizer is seeded with monodisperse seeds with initial mass per unit volume of suspension m_s and length x_0, the initial seed crystal size distribution is given by:

$$f_0(L) = \frac{m_s}{\rho_c k_v x_0^3} \delta(L - x_0) \tag{17}$$

where $m_s/\rho_c k_v x_0^3$ is the number of seed crystals per unit volume of suspension and $\delta(x)$ is the Dirac delta function with the usual properties and the units of 1/length. In our dimensionless model, the initial size distribution is given by:

$$f_0'(L') = \frac{m_s'}{x_0'^3} \delta(L' - x_0') \tag{18}$$

In 1971 Mullin and Nyvlt[6] published a concentration trajectory for seeded batch crystallization that will give a

constant crystal growth rate in the absence of nucleation. In our dimensionless framework, the trajectory is given by:

$$C'(t') = 1 - \frac{\left((1+at')^3 - 1\right)}{\left((1+a)^3 - 1\right)} \tag{19}$$

where:

$$a = \left(\frac{1}{m'_s} + 1\right)^{\frac{1}{3}} - 1 \tag{20}$$

Although the Mullin-Nyvlt trajectory (Eq. 19) is approximate (because in reality there will be some nucleation), it has the great advantage that it can be determined knowing only the mass of seeds at the beginning of the batch, the initial and final concentration, and the batch time. (Note that m'_s and C' are defined with respect to the difference between the initial and final concentration and do not depend on the kinetic parameters.) Thus if it can give results that are nearly as good as an optimal trajectory, it would be preferred because of its simplicity. The saturation concentration trajectory can be converted to a temperature trajectory if solubility data are available, and the temperature trajectory can be followed via a temperature control feedback loop.

In actual laboratory or industrial practice, it is a temperature trajectory that must be specified. If a desired saturation concentration trajectory is known, the corresponding temperature trajectory can be calculated if the solubility of the solute is known over the temperature range of interest. The Mullin-Nyvlt and linear saturation-concentration trajectories are of this form, i.e. the desired saturation concentration as a function of time is known or assumed. However, in some cases it is desirable to specify the supersaturation or crystal growth rate as a function of time instead. If this is the case, and a mathematical model for the kinetics of nucleation and growth is available, then the engineer can "back out" or "reverse engineer" the mathematical model to identify the corresponding optimal saturation concentration trajectory. This is the method that is employed to implement the constant crystal growth rate trajectory and the optimal trajectory.

Thus, given x'_0, m'_s and γ, we identify the continuous function $G'(t')$ over the interval $0 \le t' \le 1$ that minimizes the third moment of the nucleus-grown crystals at the end of the batch, $\mu'_{3,n}(t'=1)$, subject to Eqs. 15 and 16 written for both the nucleus-grown and seed-grown crystals separately and a constraint corresponding to a production rate requirement. This is accomplished by approximating the growth trajectory with a linear spline to reduce the optimization problem to a finite dimension, and solving the optimal values by iterating over the values sequentially, adjusting each point in turn until the overall function is minimized. Although there can be no guarantee that this strategy will locate the global minimum, the procedure was always found to converge to the same optimum value for many different initial conditions.

The optimal trajectory is calculated without restricting the crystal growth rate, i.e. the only requirement is that the crystal growth rate be greater than or equal to zero at all times. This corresponds to the "best case" scenario for the optimal trajectory. If there was an upper bound on the crystal growth rate (i.e. the metastable zone boundary) the optimal trajectory would perform even worse.

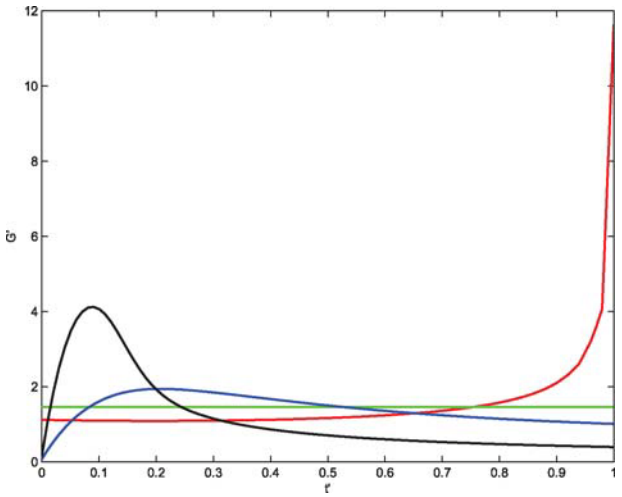

Figure 1. Growth rate versus time for four trajectories: ——— optimal trajectory; ——— constant growth rate trajectory; ——— Mullin-Nyvlt trajectory; ——— linear concentration trajectory.

[Color figure can be viewed in the online issue, which is available at wileyonlinelibrary.com.]

Results and Discussion

We present results for a particular set of parameters first, hereafter called the "base case" and then discuss, how results vary as parameters are changed. The base case values of parameters are: $x'_0 = 1$, $w' = 0.1$, $m'_s = 0.05$ and $\gamma = 3$. (w' is the dimensionless width of the parabolic CSD as described in the web-published supplement) For each set of parameters, we solve the optimal growth trajectory and compare the results with three sub-optimal trajectories: the constant growth rate trajectory, the Mullin-Nyvlt trajectory, and a linear concentration-time trajectory.

Figure 1 shows the dimensionless crystal growth rate versus dimensionless time for these four policies. The optimal crystal growth rate trajectory is nearly constant over most of the batch but increases rapidly toward the end of the batch. The constant crystal growth rate trajectory is by definition constant over the length of the batch. The Mullin-Nyvlt trajectory results in a growth rate trajectory with a broad peak early in the batch and a gradual decrease over the remainder of the batch. The linear concentration trajectory results in a more pronounced peak earlier in the batch and a steeper drop-off later in the batch.

Figure 2 shows the concentration trajectories for the same four policies. Compared with the others, the optimal trajectory decreases more abruptly toward the end of the batch, reflecting the fact that the growth rate should be greater at that time. The Mullin-Nyvlt trajectory is close to the constant growth rate trajectory but somewhat less curved. The linear concentration trajectory is (of course) nearly straight. (A small deviation from the true linear trajectory early in the batch can be observed by careful inspection of Figure 2. This is because the linear trajectory is a poor choice, and

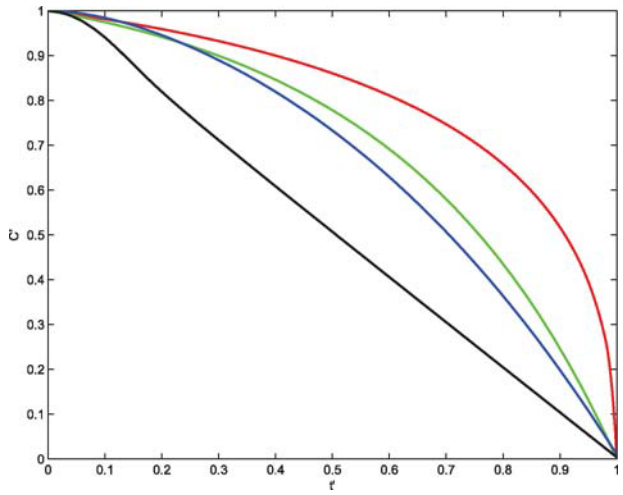

Figure 2. Concentration versus time for four trajectories: —— optimal trajectory; —— constant growth rate trajectory; —— Mullin-Nyvlt trajectory; —— linear concentration trajectory.

[Color figure can be viewed in the online issue, which is available at wileyonlinelibrary.com.]

forcing the batch to conform exactly to the linear trajectory results in computational difficulties at beginning of the batch. This deviation has negligible impact on the results.)

Figure 3 shows the time evolution of the moments (0–3) of the crystal size distribution for both the nucleus-grown (top row) and seed-grown (bottom row) crystals. The optimal supersaturation trajectory causes a dramatic increase in the number of nuclei at the very end of the batch when the growth rate increases dramatically (upper left in Figure 3). However, because this occurs at the end of the batch, the nuclei do not have a chance to grow to an appreciable size, and the volume or mass of nucleated material is the least for the optimal trajectory (upper right). In the lower left of Figure 3, the number of seed-grown crystals does not change with time because no additional seeds are added or generated. In the lower right, it can be seen that the optimal trajectory indeed achieves a greater volume or mass of seed-grown crystals at the end of the batch than any of the alternatives, followed by the constant growth trajectory, the Mullin-Nyvlent trajectory, and the linear trajectory. The final dimensionless third moment of the seed-grown CSD for these cases is 0.790, 0.747, 0.709, and 0.522, respectively.

This result is significant because it shows that the Mullin-Nyvlt trajectory performs nearly as well as the optimal trajectory, whereas the linear trajectory performs much worse. Put another way, compared to the linear trajectory, the optimal trajectory seems to do much better (a 51% improvement), however, compared to the Mullin-Nyvlt trajectory the improvement is far more modest (11%). As the Mullin-Nyvlt trajectory can be calculated without the benefit of a kinetic model, there is no reason not to use the Mullin-Nyvlt

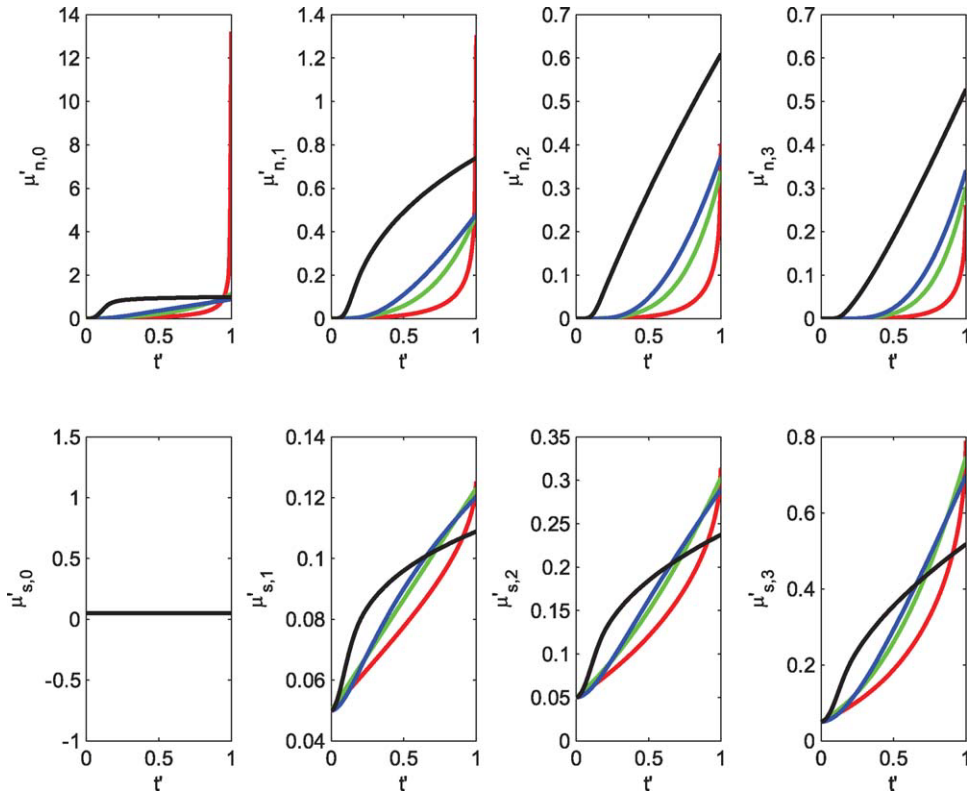

Figure 3. Moments versus time for base case. —— optimal trajectory; —— constant growth rate trajectory; —— Mullin-Nyvlt trajectory; —— linear concentration trajectory.

[Color figure can be viewed in the online issue, which is available at wileyonlinelibrary.com.]

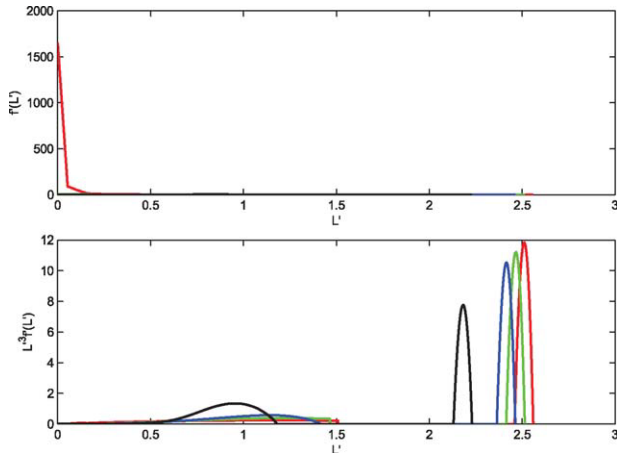

Figure 4. Crystal size distribution for the base case. —— optimal trajectory; —— constant growth rate trajectory; —— Mullin-Nyvlt trajectory; —— linear concentration trajectory.

[Color figure can be viewed in the online issue, which is available at wileyonlinelibrary.com.]

trajectory and the true benefit of developing and optimizing a kinetic model is seen by comparison of the results from the Mullin-Nyvlt trajectory with the optimal trajectory, not the linear trajectory with the optimal trajectory. In spite of this, most researchers that publish optimized trajectories compare their results with the results from a linear concentration profile.

Finally, Figure 4 shows the crystal size distribution function $f'(L')$ and the quantity $(L')^3 f'(L')$ versus L' for the four trajectories at the end of the batch. Recall that $\int_a^b f'(L')dL'$ gives the number of crystals with size between a and b, and $\int_a^b (L')^3 f'(L')dL'$ gives the volume (proportional to the mass) of crystals with size between a and b. The parabolic peaks at the right of both graphs correspond to the seeds, and the graph features at lower values of the dimensionless length correspond to nucleated crystals. The further to the right that a given peak has shifted, the greater the growth of the seed crystals and the greater the mass of the seed-grown crystals at the end of the batch. The linear concentration trajectory produces many nuclei early in the batch that have an opportunity to grow to a large size, which "steals" mass away from the seed crystals, resulting in a reduced seed-grown crystal mass. Conversely, the late-growth trajectory produces an enormous number of nuclei (notice that the CSD extends off of the graph in the upper figure) but these nuclei are produced late in the batch and do not have a chance to grow to a significant size. Thus the seed-grown crystal mass is maximized. The constant-growth and Mullin-Nyvlt trajectories fall in between these two extremes.

This analysis can be repeated for various values of x_0' and m_s'. Figure 5 shows the optimal crystal growth rate trajectory versus time for different values of x_0' and m_s'. x_0' increases from 0.5 to 1.0 and 1.5 moving down in the figure, and m_s' increases from 0.01 to 0.05 and 0.10 moving right across the

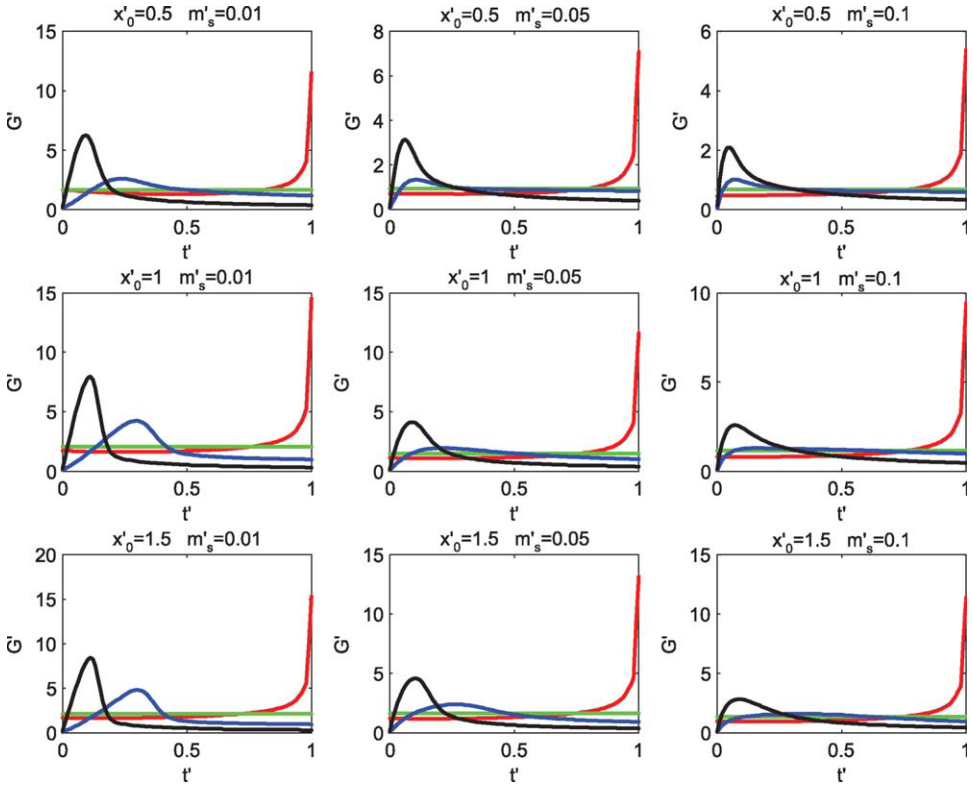

Figure 5. Growth trajectories for nine cases with $\gamma = 3$, $w' = 0.1$. —— optimal trajectory; —— constant growth rate trajectory; —— Mullin-Nyvlt trajectory; —— linear concentration trajectory.

[Color figure can be viewed in the online issue, which is available at wileyonlinelibrary.com.]

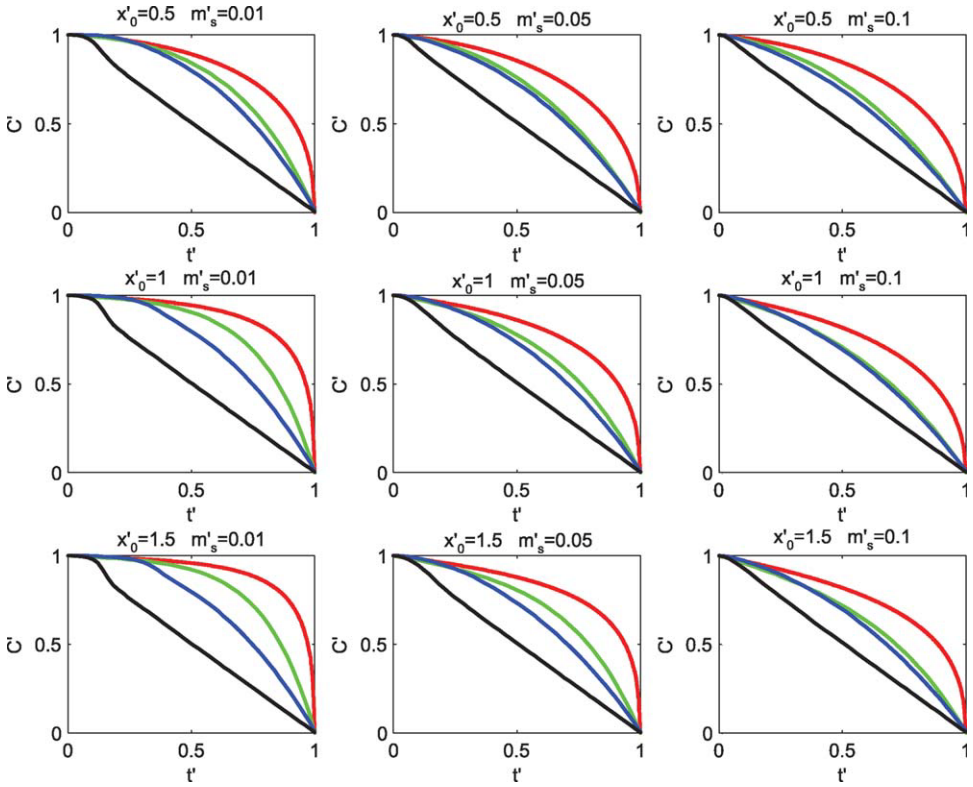

Figure 6. Concentration trajectories for nine cases with $\gamma = 3$, $w' = 0.1$. —— optimal trajectory; —— constant growth rate trajectory; —— Mullin-Nyvlt trajectory; —— linear concentration trajectory.

[Color figure can be viewed in the online issue, which is available at wileyonlinelibrary.com.]

figure. Thus seed properties are most favorable in the upper right hand corner (large seed mass and small average size) and least favorable in the lower left hand corner (small seed mass and large average size). The qualitative shape of the trajectory is the same in all instances. The major difference is the height of the spike toward the end of the batch. The spike is greatest in magnitude if the average seed size is large and/or the mass of seeds is small. This corresponds to the least favorable seed properties. The spike becomes less pronounced as the seed mass is increased or the average seed size is decreased.

Figure 6 shows the corresponding concentration trajectories for the same values of x_0' and m_s'. The best result (the lowest value of the nucleated mass at the end of the batch) occurs when the mass of seeds is the largest and the average seed size is the smallest. This corresponds to the upper right corner of Figure 6.

Generally, as the nucleated mass increases, both the optimal trajectory and the constant growth rate trajectory become more curved (less linear). Also, as the nucleated mass decreases, the constant growth trajectory approaches the Mullin-Nyvlt trajectory. This is expected, because the Mullin-Nyvlt trajectory is derived to give the constant growth-rate trajectory for the case of no nucleation. For the case where nucleation is significant, the actual constant-growth rate trajectory is more curved than that predicted by the analysis of Mullin and Nyvlt.

Figure 7 shows the time evolution of the third moment of the seed grown crystals for the same values of x_0' and m_s'. It is desired that this value be as large as possible at the end of the batch. In the upper right hand corner of the figure, where the seed properties are most favorable, all trajectories achieve a good result. Conversely, in the lower left corner, where seed properties are least favorable, all trajectories do poorly, although the optimal trajectory and constant growth trajectory do somewhat better than the Mullin-Nyvlt trajectory, which in turn does somewhat better than the linear concentration trajectory. For intermediate seed properties (the diagonal from the upper left to the lower right) the greatest benefit is seen from optimizing the growth trajectory, and the greatest penalty is paid for using the undesirable linear concentration trajectory.

This result is significant for two reasons. First, it shows that seed properties have a profound effect on the results. This has been reported before, but it is shown more clearly here because these results are system-independent. Secondly, it is clearly seen that in the case of intermediate seed loading, where the effect of the saturation concentration trajectory is most pronounced, the Mullin-Nyvlt trajectory performs nearly as well as the optimal trajectory, and the linear trajectory lags far behind. Thus if the optimal trajectory is compared with the linear saturation concentration trajectory, optimization seems to be very important and beneficial, whereas if it is compared with the Mullin-Nyvlt trajectory, the benefit is much less.

Finally, Figure 8 shows the quantity $(L')^3 f'(L')$ versus L' for the same values of x_0' and m_s'. In the upper right corner of the diagram, where the seed properties are most

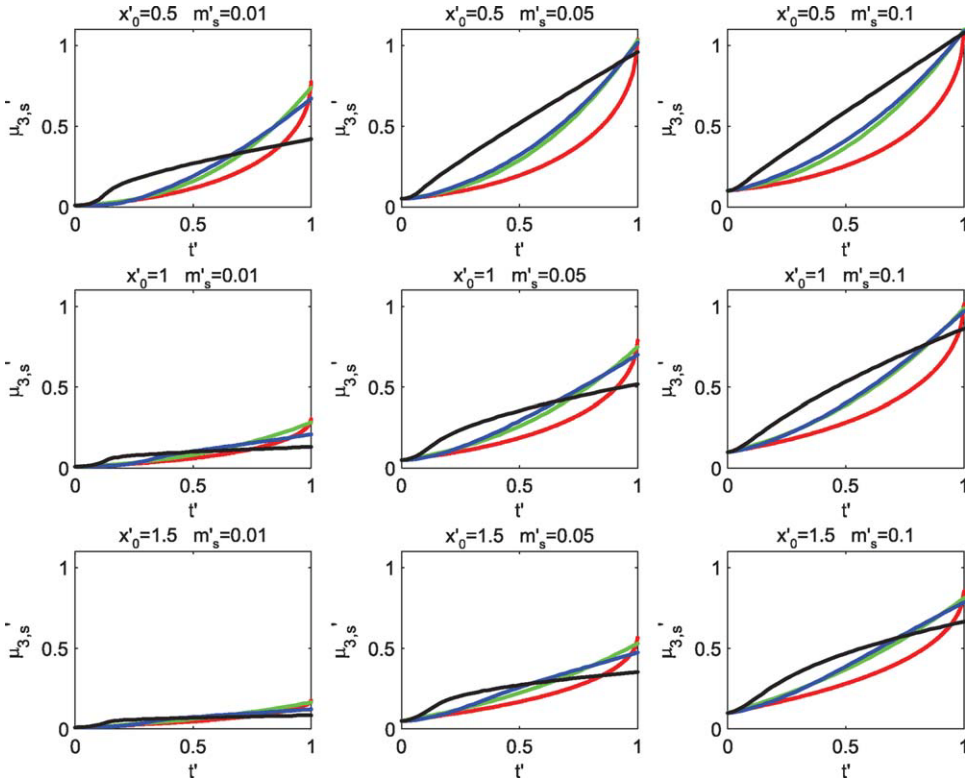

Figure 7. Time evolution of the third moment of the seed-grown crystals with $\gamma = 3$, $w' = 0.1$. —— optimal trajectory; —— constant growth rate trajectory; —— Mullin-Nyvlt trajectory; —— linear concentration trajectory.

[Color figure can be viewed in the online issue, which is available at wileyonlinelibrary.com.]

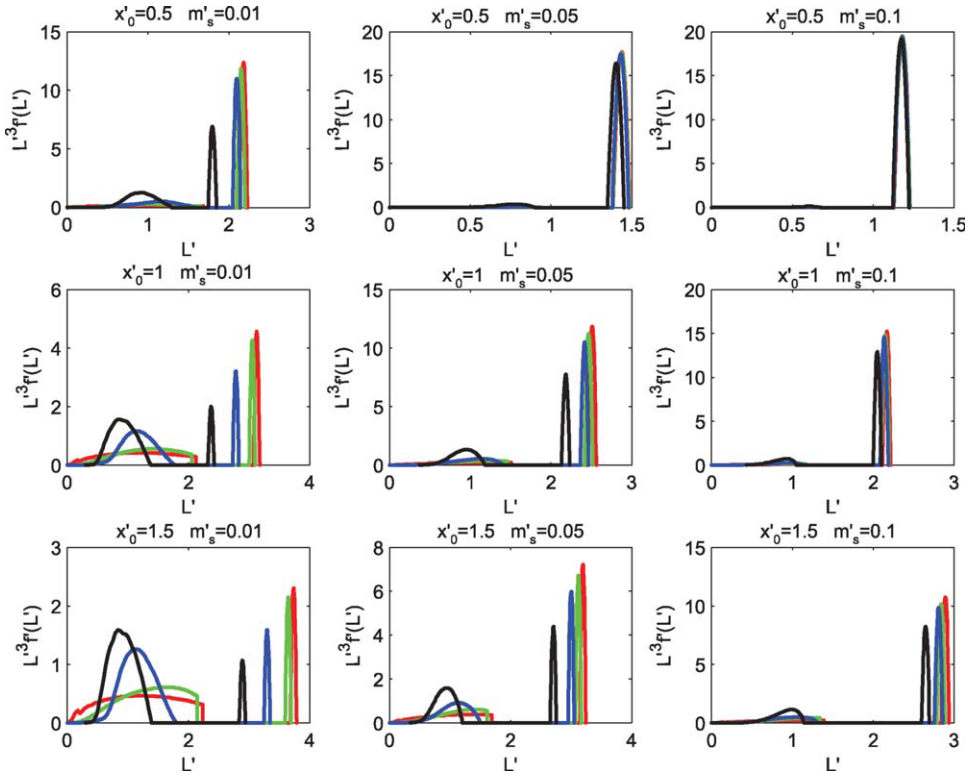

Figure 8. $(L')^3 f'(L')$ for nine cases with $\gamma = 3$, $w' = 0.1$. —— optimal trajectory; —— constant growth rate trajectory; —— Mullin-Nyvlt trajectory; —— linear concentration trajectory.

[Color figure can be viewed in the online issue, which is available at wileyonlinelibrary.com.]

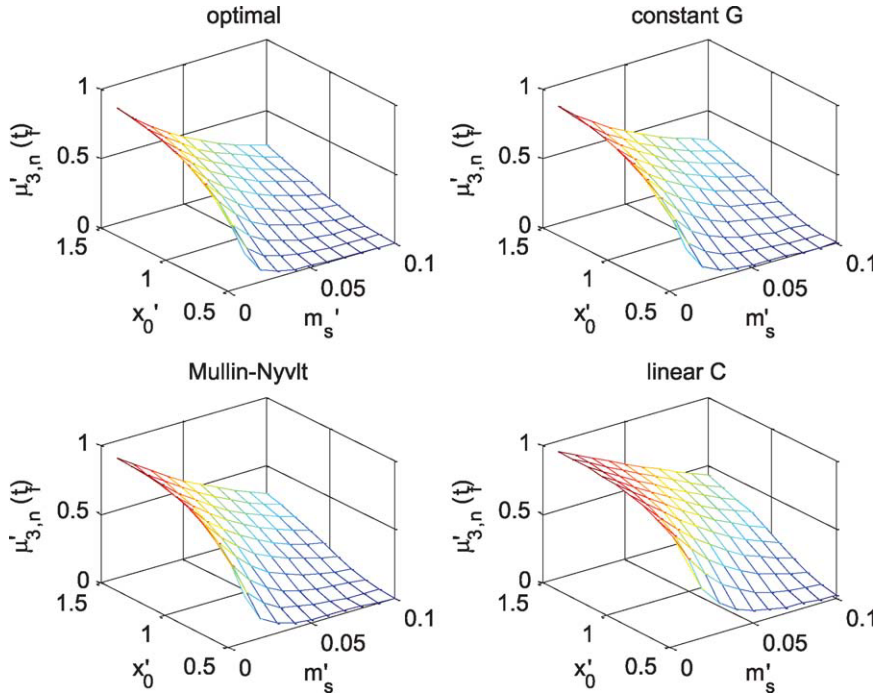

Figure 9. Dimensionless nucleated mass as a function of dimensionless total seed mass and average seed size for four different growth rate/saturation concentration trajectories: the optimal growth rate trajectory, a constant growth rate trajectory, a linear saturation concentration trajectory, and the concentration trajectory predicted by the analysis of Mullin and Nyvlt ($\gamma = 3$, $w' = 0.1$).

[Color figure can be viewed in the online issue, which is available at wileyonlinelibrary.com..]

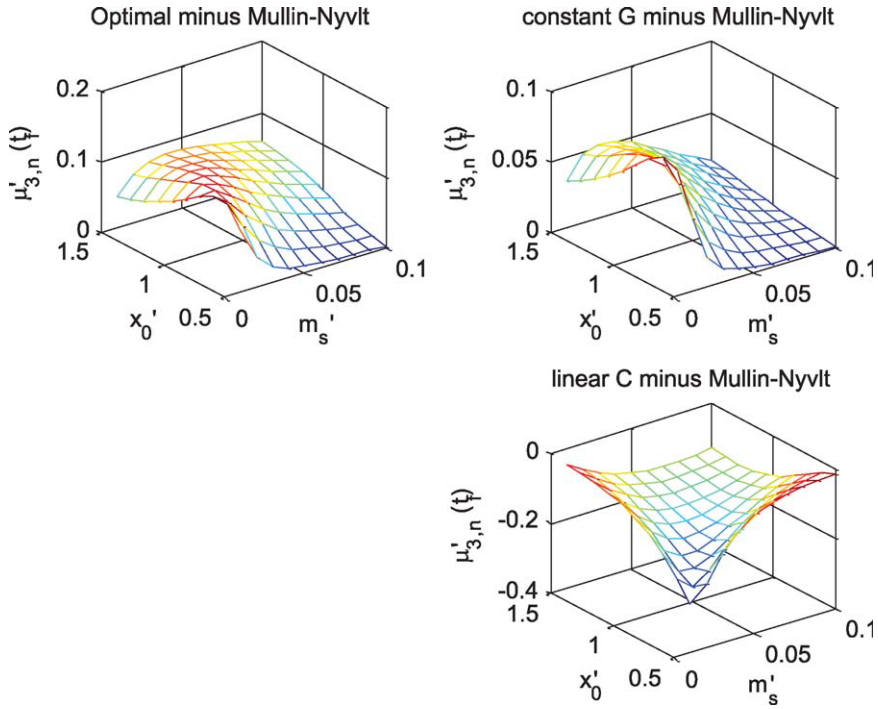

Figure 10. Difference in dimensionless nucleated mass as a function of dimensionless total seed mass and average seed size for three cases: constant growth minus optimal growth, Mullin-Nyvlt minus optimal growth, and linear minus optimal growth ($\gamma = 3$, $w' = 0.1$).

[Color figure can be viewed in the online issue, which is available at wileyonlinelibrary.com.]

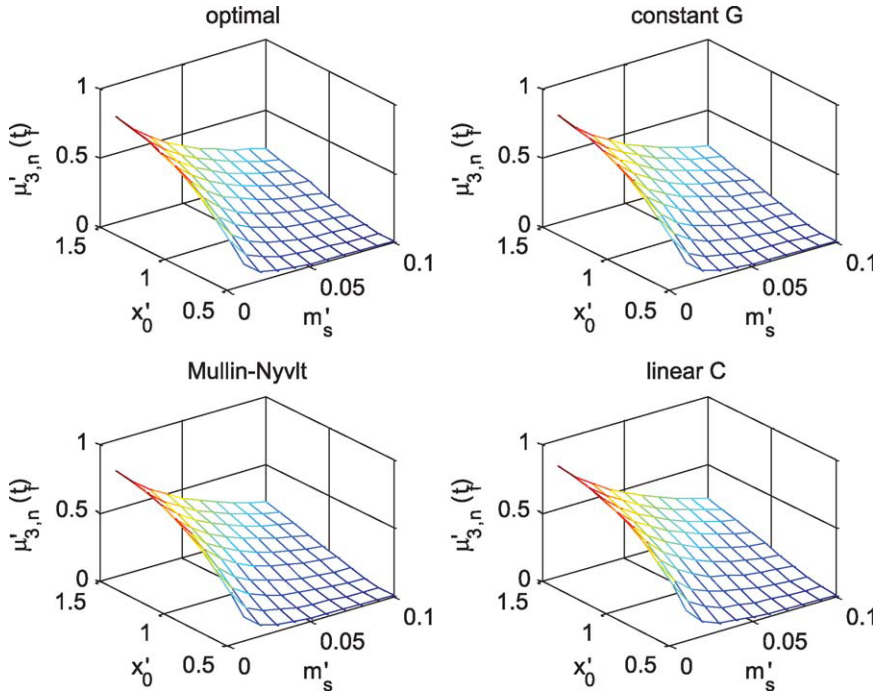

Figure 11. Dimensionless nucleated mass as a function of dimensionless total seed mass and average seed size for $\gamma = 1.5$ for four different growth rate/saturation concentration trajectories: the optimal growth rate trajectory, a constant growth rate trajectory, a linear saturation concentration trajectory, and the concentration trajectory predicted by the analysis of Mullin and Nyvlt ($w' = 0.1$).

[Color figure can be viewed in the online issue, which is available at wileyonlinelibrary.com.]

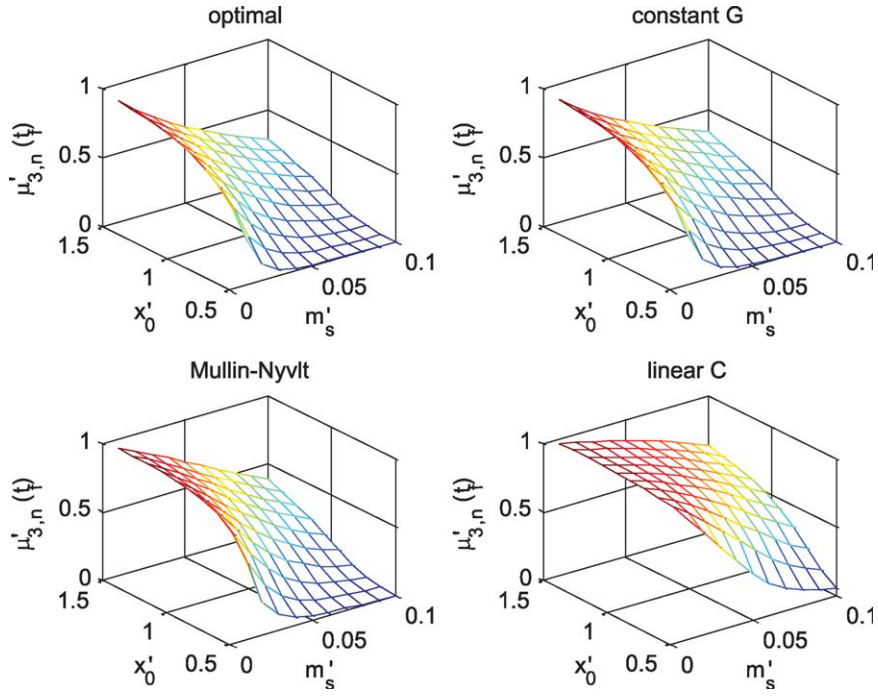

Figure 12. Dimensionless nucleated mass as a function of dimensionless total seed mass and average seed size for $\gamma = 5$ for four different growth rate/saturation concentration trajectories: the optimal growth rate trajectory, a constant growth rate trajectory, a linear saturation concentration trajectory, and the concentration trajectory predicted by the analysis of Mullin and Nyvlt ($w' = 0.1$).

[Color figure can be viewed in the online issue, which is available at wileyonlinelibrary.com.]

favorable, all trajectories produce very little nucleated mass and almost all of the mass is dedicated to the growth of seeds. Therefore the four functions lie nearly on top of one another. Conversely, in the lower left, a significant amount of mass is consumed by nucleus-grown crystals, and the growth of seeds is consequently diminished. The nucleated mass is also significantly different for different trajectories, with the linear trajectory producing the greatest amount of nucleated mass, followed by the Mullin-Nyvlt trajectory, and the constant growth trajectory. The optimal trajectory does the best.

Figure 9 shows the value of the objective function versus two seed properties, average seed size and total mass of seeds, for four different trajectories: the optimal growth trajectory, a constant growth trajectory, a linear growth trajectory and the Mullin-Nyvlt trajectory. Note that $\mu'_{3,nf} = 1$ is the worst possible outcome: all of the solute crystallized out of solution has contributed to the nucleated mass, and the seeds have not grown at all. Conversely, $\mu'_{3,nf} = 0$ is the best possible outcome: all of the solute crystallized out of solution has contributed to the growth of seeds, and none has contributed to nucleated mass. From the diagrams, it is clear that seed properties have a profound effect on the outcome of the batch. If the seed properties are poor, optimization of the supersaturation trajectory can only make a marginal improvement in the outcome. Likewise, if the seed properties are excellent, even the very poor linear trajectory gives an acceptable result. For comparison, Figure 10 shows the difference in achieved objective between the Mullin-Nyvlt trajectory and the other three trajectories. The optimal supersaturation trajectory achieves at most a 12 percentage point improvement in the mass of seed-grown material compared with the Mullin-Nyvlt trajectory, and will achieve much less than that if the seed properties are optimized. The constant growth rate trajectory achieves at most an 8.6% point improvement in the objective, and again the improvement is much less than that if the seed properties are optimized. The linear trajectory fares quite poorly for all but the best seed properties and may be as much as 26% points worse than the Mullin-Nyvlt trajectory. However, there is no compelling reason to use the linear trajectory because the Mullin-Nyvlt trajectory can be calculated knowing only the initial and final batch concentrations, the mass of seeds and the batch time.

The analysis can also be repeated for different values of the nucleation exponent γ. Figures 11 and 12 show the same information as Figure 9 but evaluated for the cases $\gamma = 1.5$, and $\gamma = 5$, respectively. For the same seed properties, decreasing the nucleation exponent reduces the nucleated mass for all trajectories. It also reduces the benefit from implementing the optimal trajectory relative to the constant growth rate trajectory or the Mullin-Nyvlt trajectory.

Conclusions

We have developed a generic dimensionless model of a seeded batch crystallization process. The model is useful because most of the physical properties of the process are eliminated in the scaling, reducing the set of parameters to a small number of dimensionless groups. As previous results of optimization of batch crystallization processes have been reported using dimensional models with all of the attendant parameters, it is difficult to compare results between different authors and draw general conclusions because the values of the parameters are different in each case. The new framework should therefore be useful to researchers who study the optimization of batch crystallization processes.

We also use the dimensionless model to compare the optimal crystal growth rate trajectory with the linear concentration trajectory, constant growth rate trajectory and the Mullin-Nyvlt trajectory for various values of seed properties and also the nucleation exponent. The fact that the process is generic allows us to draw some general conclusions:

- A constant growth rate trajectory is not the optimal growth rate trajectory for minimizing the nucleated mass at the end of the batch. Rather, the optimal growth rate trajectory is nearly flat over most of the batch, but rises rapidly toward the end of the batch.
- In spite of the previous point, a constant growth rate trajectory or even the Mullin-Nyvlt approximation to the constant growth rate trajectory may give a result that is "good enough" if seed properties are also favorable.
- Seed properties are more important than the supersaturation trajectory in the sense that optimizing the supersaturation trajectory will have a limited benefit if the seed properties are poor, but optimizing the seed properties will make a good result likely even if the supersaturation trajectory is poor.
- Nevertheless, the prudent engineer will consider both properties. The Mullin-Nyvlt trajectory can be implemented without any knowledge of the crystallization kinetics and without conducting a numerical optimization. For rapid process development, we recommend that the Mullin-Nyvlt trajectory be used and if process performance is not acceptable we recommend seeking improved performance by improving seed properties.
- The linear saturation concentration trajectory and the natural cooling trajectory are far away from the optimal trajectory and are likely to lead to a poor result unless the seed properties are excellent. As the Mullin-Nyvlt trajectory can be implemented without any additional process information beyond the initial and final concentrations, the seed mass and the batch time, the Mullin-Nyvlt trajectory should always be preferred. We recommend that researchers who investigate the optimization of batch crystallization processes should use the Mullin-Nyvlt trajectory as a benchmark, not a linear or natural cooling trajectory.

Notation

B = nucleation rate (#/(m^3 s))
f = crystal size distribution function (#/m^3 m)
G = crystal growth rate (m/s)
g = growth parameter (dimensionless)
k_b = nucleation parameter (1/(m^3 s)(m/s)$^{-\gamma}$
k_g = growth parameter (m/s)(kg/m^3)$^{-g}$
k_v = volumetric shape factor (dimensionless)
C = concentration (kg/m^3)
S = supersaturation (kg/m^3)
γ = nucleation parameter (dimensionless)
μ_i = ith moment of the crystal size distribution (m^i/m^3)
ρ = crystal density (kg/m^3)

Notes: an overbar indicates a dimensional reference quantity and a prime indicates a dimensionless quantity. Variables are made dimensionless by dividing by the reference quantity, i.e. $G' = G/\overline{G}$. When it is necessary to distinguish moments of the seed-grown crystals from moments of nucleus-grown crystals, a double subscript is employed with the letter 's' or 'n' respectively together with the moment number, i.e. $\mu_{n,3}$ is the third moment of the nucleus-grown crystals.

Literature Cited

1. Jones AG. Optimal operation of a batch cooling crystallizer. *Chem Eng Sci*. 1974;29:1075–1087.
2. Rawlings JB, Miller SM, Witkowski WR. *Ind Eng Chem Res*. 1993;32:1275–1296.
3. Ward JD, Mellichamp DA, Doherty MF. Choosing an operating policy for seeded batch crystallization. *AIChE J*. 2006;52:2046–2054.
4. Vollmer U, Raisch J. Control of batch crystallization - A system inversion approach. *Chem Eng Process*. 2006;45:874–885.
5. Vollmer U, Raisch J. Control of batch cooling crystallization processes based on orbital flatness. *Int J Control*. 2003;76:1635–1643.
6. Mullin JW, Nývlt J. Programmed cooling of batch crystallizers. *Chem Eng Sci*. 1971;26:369–377.
7. Chung SH, Ma DL, Braatz RD. Optimal seeding in batch crystallization. *Can J Chem Eng*. 1999;77:590–596.
8. Jagadesh D, Kubota N, Yokota M, Sato A, Tavare NS. Large and mono-sized product crystals from natural cooling mode batch crystallizer. *J Chem Eng Jpn*. 1996;29:865–873.
9. Kubota N, Doki N, Yokota M, Jagadesh D. Seeding effect on product crystal size in batch crystallization. *J Chem Eng Jpn*. 2002;35:1063–1071.
10. Hulburt HM, Katz S. Some problems in particle technology: a statistical mechanical formulation. *Chem Eng Sci*. 1964;19:555–574.
11. Mersmann A. editor. *Crystallization Technology Handbook*. New York: Marcel Dekker, 2001.
12. Nyvlt, J. *Design of Crystallizers*. Boca Raton, FL: CRC Press, 1992.
13. Ramkrishna D. *Population Balances*. San Diego: Academic Press, 2000.
14. Randolph AD, Larson MA. *Theory of Particulate Processes*. New York: Academic Press, 1988.
15. Tavare NS. *Industrial Crystallization: Process Simulation Analysis and Design*. New York: Plenum Press, 1995.

Manuscript received Apr. 3, 2009, and revision received Mar. 20, 2010.